Inorg. Chem. **2004**, *43*, 7075–7082

Supramolecular Copper Hydroxide Tennis Balls: Self-Assembly, Structures, and Magnetic Properties of Octanuclear $[Cu_8L_8(OH)_4]^{4+}$ Clusters (HL = *N*-(2-Pyridylmethyl)acetamide)

Arunendu Mondal,[†] Yang Li,[‡] Masood A. Khan,[†] Joseph H. Ross, Jr.,*[,‡] and Robert P. Houser*[,†]

Department of Chemistry and Biochemistry, University of Oklahoma, 620 Parrington Oval, Norman, Oklahoma 73019, and Department of Physics, Texas A&M University, College Station, Texas 77843

Received May 24, 2004

The self-assembly of supramolecular copper "tennis balls" that possess unusual magnetic properties using a small pyridyl amide ligand is described. Copper(II) complexes of *N*-(2-pyridylmethyl)acetamide (HL) were synthesized in methanol. In the absence of base, the mononuclear complex $[Cu(HL)_2](ClO_4)_2$ (**1**) was prepared. The structure of **1**, determined by X-ray crystallography, contains a copper(II) ion surrounded by bidentate HL ligands coordinated via the pyridyl N atom and the carbonyl O atom in a trans, square planar arrangement. Reactions carried out in the presence of triethylamine resulted in cluster complexes $[Cu_8L_8(OH)_4](ClO_4)_4$ and $[Cu_8L_8(OH)_4](CF_3SO_3)_4$ [**2**$(ClO_4)_4$ and **2**$(OTf)_4$, respectively]. The cationic portions of **2**$(ClO_4)_4$ and **2**$(OTf)_4$ are isostructural, containing eight copper(II) ions, eight deprotonated ligands (L^-), and four μ_3-hydroxide ligands. The top and bottom halves of the cluster are related by a pseudo-S_4 symmetry operation and are held together by bridging L^- ligands. Solutions of **2**$(ClO_4)_4$ and **2**$(OTf)_4$, which were shown to contain the full $[Cu_8L_8(OH)_4]^{4+}$ fragment by electrospray mass spectrometry and conductance experiments, are EPR silent. Magnetic susceptibility measurements for **2**$(ClO_4)_4$ as a function of temperature and magnetic field showed the Cu ions all to exhibit magnetic moments in the range expected for the d^9 configuration. At low temperatures, the magnetization was reduced due to predominantly antiferromagnetic interactions between ions. Analysis showed that partially frustrated interactions among the four Cu ions making up each half of the cluster gave good agreement with the data once a large molecular anisotropy was taken into account, with $J_c = 106$ cm^{-1}, $D = 27$ cm^{-1}, and $g = 2.17$.

Introduction

Multinuclear metal clusters are ubiquitous to many areas of chemistry and biochemistry, including main group and organometallic chemistry,[1] lanthanide chemistry,[2] and bioinorganic chemistry.[3] Particular interest in polynuclear copper complexes has been sparked in recent years by the characterization of several unusual metalloenzymes that contain copper clusters, including particulate methane monooxygenase (pMMO)[4] and nitrous oxide reductase (N_2OR).[5] Although the structure of the copper cluster in pMMO has yet to be established due to difficulties in purifying the membrane-bound enzyme, the structure of the so-called Cu_Z active site of N_2OR was recently elucidated as a μ_4-sulfide bridged tetranuclear copper cluster.[6] N_2OR catalyzes the two-electron reduction of nitrous oxide to dinitrogen in the terminal step of the denitrification pathway found in anaerobic soil bacteria.[7] Recently, Solomon and co-workers have probed

* To whom correspondence should be addressed. E-mail: houser@ou.edu (R.P.H.); jhross@tamu.edu (J.H.R.).
[†] University of Oklahoma.
[‡] Texas A & M University.

(1) (a) Roesky, H. W.; Haiduc, I.; Hosmane, N. S. *Chem. Rev.* **2003**, *103*, 2579−2595. (b) Whitmire, K. H. *Adv. Organomet. Chem.* **1998**, *42*, 1−145.
(2) Bunzli, J.-C. G.; Piquet, C. *Chem. Rev.* **2002**, *102*, 1897−1928.
(3) Rao, P. V.; Holm, R. H. *Chem. Rev.* **2004**, *104*, 527−559.
(4) Lieberman, R. L.; Shrestha, D. B.; Doan, P. E.; Hoffman, B. M.; Stemmler, T. L.; Rosenzweig, A. C. *Proc. Natl. Acad. Sci. U.S.A.* **2003**, *100*, 3820−3825.
(5) Brown, K.; Djinovic-Carugo, K.; Haltia, T.; Cabrito, I.; Saraste, M.; Moura, J. J. G.; Moura, I.; Tegoni, M.; Cambillau, C. *J. Biol. Chem.* **2000**, *275*, 41133−41136.
(6) (a) Brown, K.; Tegoni, M.; Prudêncio, M.; Pereira, A. S.; Besson, S.; Moura, J.; Moura, I.; Cambillau, C. *Nat. Struct. Biol.* **2000**, *7*, 191−195. (b) Rasmussen, T.; Berks, B. C.; Sanders-Loehr, J.; Dooley, D. M.; Zumft, W. G.; Thomson, A. J. *Biochemistry* **2000**, *39*, 12753−12756. (c) Chen, P.; Cabrito, I.; Moura, J. J. G.; Moura, I.; Solomon, E. I. *J. Am. Chem. Soc.* **2002**, *124*, 10497−10507.

10.1021/ic0493292 CCC: $27.50
Published on Web 09/28/2004

the spectroscopic properties of Cu_Z and have suggested that the active form is in the fully reduced $4Cu^I$ state.[8] The unresolved mechanism and the paucity of synthetic analogues of this unique copper sulfide cluster has led us and others to pursue the goal of modeling the Cu_Z site.[9]

Another source of interest into copper clusters resides in the inherent magnetic complexity that is possible in these complexes. Numerous examples of magnetic exchange in oxo- and hydroxo-bridged copper(II) binuclear and polynuclear complexes have been reported.[10] For the family of hydroxo-bridged binuclear copper(II) complexes, the singlet−triplet energy gap, J, is linearly dependent on the Cu−O−Cu bond angle, θ, having a singlet ground state when $\theta > 97.5°$ and a triplet ground state when $\theta < 97.5°$.[11] The relationship between Cu−OH−Cu bond angle and the degree and type of magnetic exchange is more complex in hydroxide-bridged multinuclear copper complexes.[12,13] In addition to hydroxide-bridged copper clusters, many examples of multinuclear copper clusters have been reported over the years, including tetranuclear and octanuclear copper complexes that do not contain hydroxide bridges.[13,14]

Multinuclear copper clusters comprise a small subset of the larger family of metal-based supramolecular assemblies. The self-assembly of supramolecular structures formed via ligand−metal coordinate bonds continues to attract considerable attention.[15] Of particular relevance to this work are the many supramolecular complexes that utilize ligands which contain a pyridyl group or groups. For example, Stang and co-workers have used ligands with directionally oriented pyridyl groups as building blocks with platinum to prepare supramolecular squares and prisms.[16] Supramolecular architectures were created by Lehn and co-workers using polypyridyl, terpyridine-type ligands, and Pb(II) ions.[17] Finally, a large number of coordination polymers have been synthesized with pyridyl-containing ligands such as nicotinate,[18] mixed pyridyl/pyrimidyl ligands,[19] or bipyridine and bipyridine-like ligands.[20]

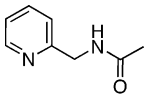

HL

Using the deceptively simple-looking ligand *N*-(2-pyridylmethyl)acetamide, HL, we have discovered the self-assembly of some remarkable supramolecular copper(II) "tennis balls". A key to the unusual chemistry of HL is its versatility regarding the manner in which it coordinates to copper(II) ions. Complexes formed with HL as is, in its neutral form, are simple mononuclear species. However, when the amide nitrogen is deprotonated, the anionic amidate ligand, L^-, forms highly symmetrical octanuclear copper(II) hydroxide clusters with approximate S_4 symmetry, the same symmetry present in a tennis ball. Here we report the syntheses of copper(II) complexes of HL and L^-, including the self-assembly, structures, and magnetic characterization of two isostructural copper(II) hydroxide clusters that contain eight copper(II) ions in a highly symmetrical arrangement.

Experimental Section

General. All reagents were purchased from commercial sources and used without further purification. Solvents were dried and purified under nitrogen using standard methods and were distilled immediately before use. ^{1}H NMR spectra were measured on a Varian 300 MHz spectrometer using solvent as an internal standard. Elemental analyses were carried out by Atlantic Microlabs, Norcross, GA. Mass spectra were recorded on a Q-TOF quadrupole time-of flight mass spectrometer (Micromass, Manchester, U.K.) equipped with a Z-spray electrospray ionization (ESI) source.

(7) (a) Coyle, C. L.; Zumft, W. G.; Kroneck, P. M. H.; Koerner, H.; Jakob, W. *Eur. J. Biochem.* **1985**, *153*, 459−467. (b) Snyder, S. W.; Hollocher, T. C. *J. Biol. Chem.* **1987**, *262*, 6515−6525. (c) SooHoo, C. K.; Hollocher, T. C. *J. Biol. Chem.* **1991**, *266*, 2203−2209.

(8) (a) Chen, P.; George, S. D.; Cabrito, I.; Antholine, W. E.; Moura, J. J. G.; Moura, I.; Hedman, B.; Hodgson, K. O.; Solomon, E. I. *J. Am. Chem. Soc.* **2002**, *124*, 744−745. (b) Ghosh, S.; Gorelsky, S. I.; Chen, P.; Cabrito, I.; Moura, J. J. G.; Moura, I.; Solomon, E. I. *J. Am. Chem. Soc.* **2003**, *125*, 15708−15709.

(9) (a) Stephens, J. C.; Khan, M. A.; Houser, R. P. *Inorg. Chem.* **2001**, *40*, 5064−5065. (b) Helton, M. E.; Chen, P.; Paul, P. P.; Tyeklár, Z.; Sommer, R. D.; Zakharov, L. N.; Rheingold, A. L.; Solomon, E. I.; Karlin, K. D. *J. Am. Chem. Soc.* **2003**, *125*, 1160−1161.

(10) (a) Melnik, M. *Coord. Chem. Rev.* **1982**, *42*, 259−293. (b) Hodgson, D. J. In *Progress in Inorganic Chemistry*; Lippard, S. J., Ed.; John Wiley & Sons: New York, 1975; Vol. 19, pp 173−241. (c) Kato, M.; Muto, Y. *Coord. Chem. Rev.* **1988**, *92*, 45−83.

(11) Crawford, V. H.; Richardson, H. W.; Wasson, J. R.; Hodgson, D. J.; Hatfield, W. E. *Inorg. Chem.* **1976**, *15*, 2107−2110.

(12) (a) Triki, S.; Thétiot, F.; Pala, J. S.; Golhen, S.; Clemente-Juan, J. M.; Gómez-García, C. J.; Coronado, E. *Chem. Commun.* **2001**, 2172−2173. (b) Gajda, T.; Dupre, Y.; Torok, I.; Harmer, J.; Schweiger, A.; Sander, J.; Kuppert, D.; Hegetschweiler, K. *Inorg. Chem.* **2001**, *40*, 4918−4927. (c) Gou, S.; Qian, M.; Yu, Z.; Duan, C.; Sun, X.; Huang, W. *J. Chem. Soc., Dalton Trans.* **2001**, 3232−3237. (d) Ferrer, S.; Haasnoot, J. G.; Reedijk, J.; Müller, E.; Cingi, M. B.; Lanfranchi, M.; Lanfredi, A. M. M.; Ribas, J. *Inorg. Chem.* **2000**, *39*, 1859−1867. (e) Matthews, C. J.; Avery, K.; Xu, Z.; Thompson, L. K.; Zhao, L.; Miller, D. O.; Biradha, K.; Poirier, K.; Zaworotko, M. J.; Wilson, C.; Goeta, A. E.; Howard, J. A. K. *Inorg. Chem.* **1999**, *38*, 5266−5276. (f) Tangoulis, V.; Raptopoulou, C. P.; Paschalidou, S.; Bakalbassis, E. G.; Perlepes, S. P.; Terzis, A. *Angew. Chem., Int. Ed.* **1997**, *36*, 1083−1085. (g) Liu, X.; McAllister, J. A.; de Miranda, M. P.; Whitaker, B. J.; Kilner, C. A.; Thornton-Pett, M.; Halcrow, M. A. *Angew. Chem., Int. Ed.* **2002**, *41*, 756−758.

(13) Mukherjee, A.; Rudra, I.; Nethaji, M.; Ramasesha, S.; Chakravarty, A. R. *Inorg. Chem.* **2003**, *42*, 463−468.

(14) (a) Tangoulis, V.; Paschalidou, S.; Bakalbassis, E. G.; Perlepes, S. P.; Raptopoulou, C. P.; Terzis, A. *Chem. Commun.* **1996**, 1297−1298. (b) Blake, A. J.; Grant, C. M.; Gregory, C. I.; Parsons, S.; Rawson, J. M.; Reed, D.; Winpenny, R. E. P. *J. Chem. Soc., Dalton Trans.* **1995**, 163−175. (c) Ardizzoia, G. A.; Angaroni, M. A.; La Monica, G.; Cariati, F.; Cenini, S.; Moret, M.; Masciocchi, N. *Inorg. Chem.* **1991**, *30*, 4347−4353. (d) McKee, V.; Tandon, S. S. *Inorg. Chem.* **1989**, *28*, 2901−2902. (e) Agostinelli, E.; Dell'Amico, D. B.; Calderazzo, F.; Fiorani, D.; Pelizzi, G. *Gazz. Chim. Ital.* **1988**, *118*, 729−740. (f) Thompson, L. K. *Coord. Chem. Rev.* **2002**, *233*−*234*, 193−206.

(15) (a) Seidel, S. R.; Stang, P. J. *Acc. Chem. Res.* **2002**, *35*, 972−983. (b) Lehn, J.-M. *Proc. Natl. Acad. Sci. U.S.A.* **2002**, *99*, 4763−4768. (c) Holliday, B. J.; Mirkin, C. A. *Angew. Chem., Int. Ed.* **2001**, *40*, 2022−2043.

(16) (a) Tabellion, F. M.; Seidel, S. R.; Arif, A. M.; Stang, P. J. *J. Am. Chem. Soc.* **2001**, *123*, 7740−7741. (b) Kryschenko, Y. K.; Seidel, S. R.; Muddiman, D. C.; Nepomuceno, A. I.; Stang, P. J. *J. Am. Chem. Soc.* **2003**, *125*, 9647−9652.

(17) Barboiu, M.; Vaughan, G.; Graff, R.; Lehn, J.-M. *J. Am. Chem. Soc.* **2003**, *125*, 10257−10265.

(18) Rather, B.; Moulton, B.; Walsh, R. D. B.; Zaworotko, M. J. *Chem. Commun.* **2002**, 694−695.

(19) Shin, D. M.; Lee, I. S.; Chung, Y. K.; Lah, M. S. *Chem. Commun.* **2003**, 1036−1037.

(20) (a) Fletcher, A. J.; Cussen, E. J.; Prior, T. J.; Rosseinsky, M. J.; Kepert, C. J.; Thomas, K. M. *J. Am. Chem. Soc.* **2001**, *123*, 10001−10011. (b) Belcher, W. J.; Longstaff, C. A.; Neckenig, M. R.; Steed, J. W. *Chem. Commun.* **2002**, 1602−1603.

Electronic absorption spectra were measured on a Shimadzu UV2401PC UV−vis spectrophotometer. IR spectra were recorded on a NEXUS 470 FTIR spectrometer using the KBr pellet technique. Conductance measurements were made using a YSI model 31A conductivity bridge as previously described.[21] X-band EPR spectra were recorded on a Bruker EMX spectrometer at 100 K as frozen solutions at ∼9.5 GHz.

CAUTION: *Perchlorate salts of metal complexes with organic ligands are potentially explosive. Although no problems were encountered in this work, only small amounts of material should be prepared and handled with caution.*

***N*-(2-Pyridylmethyl)acetamide (HL).** The synthesis of HL was carried out via a modified procedure based upon a published method.[22] 2-(Aminomethyl)pyridine (1.08 g, 10 mmol) and acetic anhydride (4.32 g, 42.3 mmol) were dissolved in 3 mL of pyridine and stirred at room temperature for 24 h, after which 4 mL of water was added with stirring for another 1 h. Solvent was removed under vacuum, leaving a brown liquid. The crude product was distilled at reduced pressure to produce a colorless liquid that solidified upon cooling, 1.05 g (70% yield). ^{1}H NMR (300 MHz, $CDCl_3$): δ = 2.04 (s, 3H); 4.54 (d, 2H); 6.95 (br s, 1H); 7.2 (m, 2H); 7.63 (t, 1H); 8.50 (d, 1H) ppm.

$[Cu(HL)_2](ClO_4)_2$ (1). A methanol solution of ligand HL (0.150 g, 1 mmol) was slowly added to a methanol solution of $Cu(ClO_4)_2\cdot 6H_2O$ (0.185 g, 0.5 mmol) with constant stirring at room temperature. The solution was stirred for 1 h, whereupon a blue precipitate formed. The precipitate was collected by filtration, washed with methanol, and dried under vacuum, 0.171 g (70% yield). Anal. Calcd for $C_{16}H_{20}Cl_2CuN_4O_{10}$: C, 34.13; H, 3.55; N, 9.95. Found: C, 34.19; H, 3.51; N, 9.89. ESI-MS (CH_3CN): m/z = 462.0 [M − ClO_4]$^+$. UV−vis [H_2O, λ_{max}, nm (ϵ, M^{-1} cm^{-1})]: 745 (20). FTIR (KBr): 1259, 1238, 3333, 3125, 3081, 1609, 1490, 1445, 1376, 1366, 1318, 1167, 1082, 1039, 969, 837, 778, 759, 657, 636, 621, 579, 531, 511, 438 cm^{-1}.

$[Cu_8L_8(OH)_4](ClO_4)_4$ [2(ClO_4)$_4$]. A methanol solution of HL (0.150 g, 1 mmol) and triethylamine (0.408 g, 4 mmol) was added to a methanol solution of $Cu(ClO_4)_2\cdot 6H_2O$ (0.370 g, 1 mmol). The solution was stirred at room temperature for 1 h, whereupon a blue precipitate formed. The precipitate was collected by filtration, washed with methanol, and dried under vacuum, 0.135 g (50% yield). Anal. Calcd for $C_{64}H_{84}Cl_4Cu_8N_{16}O_{28}$: C, 35.46; H, 3.53; N, 10.34. Found: C, 35.12; H, 3.57; N, 10.38. ESI-MS (CH_3CN): m/z = 2066.6 [M − ClO_4]$^+$; 441.0 [$Cu_2L_2(OH)$]$^+$. UV−vis [CH_3CN, λ_{max}, nm (ϵ, mol^{-1} cm^{-1})]: 304 (5200), 638 (410). FTIR (KBr): 3437, 1612, 1581, 1561, 1487, 1427, 1354, 1283, 1221, 1160, 1088, 1027, 903, 769, 721, 667, 623, 588 cm^{-1}.

$[Cu_8L_8(OH)_4](CF_3SO_3)_4$ [2(OTf)$_4$]. A methanol solution of HL (0.150 g, 1 mmol) and triethylamine (0.408 g, 4 mmol) was added to a methanol solution of $Cu(CF_3SO_3)_2$ (0.361 g, 1 mmol). The solution was stirred at room temperature for 1 h, whereupon a blue precipitate formed. The precipitate was collected by filtration, washed with methanol, and dried under vacuum, 0.120 g (45% yield). Anal. Calcd for **2**(OTf)$_4\cdot CH_3CN$, $C_{70}H_{79}Cu_8F_{12}N_{17}O_{24}S_4$: C, 34.93; H, 3.31; N, 9.89. Found: C, 34.99; H, 3.30; N, 9.98. ESI-MS (CH_3CN): m/z = 2214.9 [M − CF_3SO_3]$^+$; 441.0 [$Cu_2L_2(OH)$]$^+$. UV−vis [CH_3CN, λ_{max}, nm (ϵ, mol^{-1} cm^{-1})]: 301 (6000), 653 (570). FTIR (KBr, cm^{-1}): 3115, 1611, 1579, 1562, 1488, 1429, 1359, 1272, 1222, 1153, 1119, 1101, 1055, 1030, 905, 767, 721, 668, 638, 573, 517.

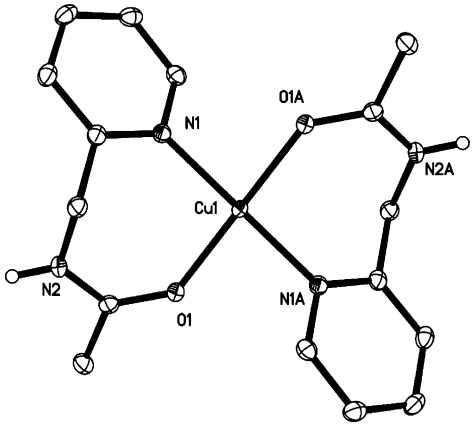

Figure 1. Thermal ellipsoid representation of the X-ray crystal structure of $[Cu(HL)_2](ClO_4)_2$ (**1**); thermal ellipsoids are drawn at the 50% level. Perchlorate anions and all H atoms except for the amide H atoms are omitted for clarity. Selected bond distances (Å) and angles (deg): Cu1−O1, 1.9560(13); Cu1−N1, 1.9981(15); O1−Cu1−O1A, 180.000(1); N1−Cu−N1A, 180.00(7); O1−Cu−N1, 94.88(6); O1−Cu1−N1A, 85.12(6).

Table 1. Crystallographic Data for **1**, **2**(ClO_4)$_4$, and **2**(OTf)$_4$

	1	**2**(ClO_4)$_4\cdot 6CH_3CN$	**2**(OTf)$_4\cdot 2CH_3CN$
formula	$C_{16}H_{20}Cl_2CuN_4O_{10}$	$C_{76}H_{94}Cl_4Cu_8N_{22}O_{28}$	$C_{72}H_{82}Cu_8F_{12}N_{18}O_{24}S_4$
fw	562.80	2413.85	2448.12
temp (K)	100(2)	120(1)	100(1)
space group	$P\bar{1}$	$P\bar{1}$	$P4_3$
a (Å)	7.7771(12)	15.385(6)	15.1881(9)
b (Å)	8.1565(13)	16.236(6)	15.1881(9)
c (Å)	8.9099(14)	23.227(9)	38.671(5)
α (deg)	74.492(2)	71.041(6)	90
β (deg)	73.952(2)	75.739(6)	90
γ (deg)	76.299(2)	63.633(6)	90
Z	1	2	4
V (Å^3)	515.22(14)	4881(3)	8920.5(13)
ρ_{calcd} (g/cm^3)	1.814	1.643	1.823
μ (mm^{-1})	1.385	1.902	2.072
R1 [$I > 2\sigma(I)$]	0.0255	0.0479	0.0190
wR2 [$I > 2\sigma(I)$]	0.0675	0.1142	0.0499
GOF on F^2	1.068	0.947	1.046

X-ray Crystal Structure Determination. Single crystals of **1**, **2**(ClO_4)$_4$, and **2**(OTf)$_4$ suitable for X-ray analysis were grown by slowly diffusing diethyl ether into acetonitrile solutions of the complexes. The data for **1**, **2**(ClO_4)$_4$, and **2**(OTf)$_4$ were collected on a Bruker Apex diffractometer with graphite-monochromated Mo Kα (λ = 0.71073 Å) radiation. The structures were solved by direct methods using the SHELXTL system,[23] and refined by full-matrix least-squares on F^2 using all reflections. Crystal data for **1**, **2**(ClO_4)$_4\cdot 6CH_3CN$, and **2**(OTf)$_4\cdot 2CH_3CN$ are summarized in Table 1. Selected bond lengths and angles are summarized for **1** in the caption of Figure 1, and selected average bond lengths and angles for for **2**(ClO_4)$_4$ and **2**(OTf)$_4$ are summarized in Table 2.

The four ClO_4 ions and the six CH_3CN solvent molecules are slightly disordered in the structure of **2**(ClO_4)$_4\cdot 6CH_3CN$. The disorder in the perchlorate anion containing Cl3 is resolved for the two components of the oxygen atoms. However, for the other perchlorate ions and the solvent molecules, it was not possible to resolve the disorder in separate components due to the close proximity of these components. Hence, relatively large thermal ellipsoids for the oxygen atoms, compared to the Cl atom to which they are bonded, are reasonable.

Magnetization and Magnetic Susceptibility. DC magnetic susceptibility measurements were performed on a powdered sample

(21) Chandra, T.; Allred, R. A.; Kraft, B. J.; Berreau, L. M.; Zaleski, J. M. *Inorg. Chem.* **2004**, *43*, 411−420.
(22) Li, C.; Rittmann, L. S.; Tsiftsoglou, A. S.; Bhargava, K. K.; Sartorelli, A. C. *J. Med. Chem.* **1978**, *21*, 874−877.
(23) Sheldrick, G. M. *SHELXTL, Version 5.1*; Bruker AXS: Madison, WI, 1997.

Table 2. Selected Average Bond Lengths (Å) and Angles (deg) for **2**$(ClO_4)_4$ and **2**$(OTf)_4$

	2$(ClO_4)_4$	**2**$(OTf)_4$
CuA−N(amide)	1.996(9)	1.973(4)
CuA−N(py)	2.010(5)	1.984(5)
CuA−O(amide)	1.95(1)	1.929(3)
CuA−OH	1.91(1)	1.881(2)
CuB−N(amide)	1.996(5)	1.973(4)
CuB−N(py)	2.00(1)	1.986(2)
CuB−O(amide)	2.04(2)	2.011(9)
CuB−OH(eq)	1.92(1)	1.906(4)
CuB−OH(ax)	2.35(5)	2.39(1)
N(py)−CuA−OH	170(4)	168(2)
N(amide)−CuA−O(amide)	168(2)	170(1)
N(amide)−CuA−N(py)	83.1(3)	83.6(2)
N(amide)−CuA−OH	95.9(4)	95.4(2)
N(py)−CuA−O(amide)	89.2(4)	89.2(3)
O(amide)−CuA−OH	92(1)	93.2(3)
N(py)−CuB−OH(eq)	171(2)	170.9(6)
N(amide)−CuB−O(amide)	151(6)	153(1)
N(amide)−CuB−N(py)	83.4(3)	83.4(1)
N(amide)−CuB−OH(eq)	97.6(9)	97.6(5)
N(py)−CuB−O(amide)	91.7(4)	92.2(4)
O(amide)−CuB−OH(eq)	91.5(5)	90.9(4)
OH(eq)−CuB−OH(ax)	79(2)	78.2(4)
N(py)−CuB−OH(ax)	92(2)	92.8(7)
N(amide)−CuB−OH(ax)	108(6)	107(2)
O(amide)−CuB−OH(ax)	100(2)	100(1)
CuA−OH−CuB	124(4)	127.7(4)
CuA−OH−CuB′	113(6)	108.8(5)
CuB−OH−CuB′	96(1)	97.9(3)

of **2**$(ClO_4)_4$ (44.39 mg) with a Quantum Design MPSP-XL SQUID magnetometer operating in the temperature range 2−300 K. The sample was held in a polyethylene bag during measurements, with the small bag diamagnetic contribution removed from the data by subtracting. DC susceptibility measurements were performed in a fixed field of 1000 Oe. The magnetization data corresponding to the zero-field-cooled (ZFC) regime were taken on heating after sample cooling at zero applied field, while magnetization in the field-cooled (FC) regime was measured as a function of decreasing temperature in the applied field. Magnetization versus applied field was also measured at 2 K in fields up to 70 kOe.

Results and Discussion

With the goal of generating complexes that model the unprecedented Cu_Z center from nitrous oxide reductase, we set out to synthesize new copper clusters. We have adopted a stepwise approach to the ultimate goal of creating a Cu_4S cluster that mimics the structure and reactivity of Cu_Z. The first step of this approach is to synthesize copper clusters into which sulfide anions will be inserted. Our strategy for the self-assembly of the copper clusters takes advantage of the anionic, bridging ligand, *N*-(2-pyridylmethyl)acetamidate (L^-). This ligand is derived from the amide, *N*-(2-pyridylmethyl)acetamide (HL), which was studied in the 1970s as a potential inducer of erythroid differentiation in Friend leukemia cells.[22] Surprisingly, to our knowledge no coordination chemistry with HL or L^- has been reported since this initial report. The deprotonated ligand acts as a template for the self-assembly of the copper hydroxide clusters due to its dual role as a chelating ligand to one metal ion through the pyridyl and amidate N ligand atoms, and coordination to a second metal ion via the carbonyl O atom. Furthermore, this carbonyl O atom can coordinate to a second metal ion in either a syn or anti sense, enabling the self-assembly of supramolecular clusters.

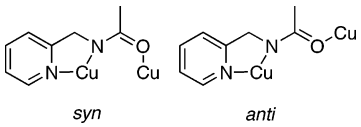

Copper complexes of HL and L^- were synthesized in methanol by treatment of a copper(II) salt with either HL alone, or with HL and a base. The importance of the base to deprotonate the amide nitrogen on HL was demonstrated by the production of the mononuclear square planar complex, $[Cu(HL)_2](ClO_4)_2$ (**1**), when HL was combined with $Cu(ClO_4)_2 \cdot 6H_2O$ in methanol in the absence of triethylamine. The structure of **1**, determined by X-ray diffraction, consists of square planar copper ions coordinated symmetrically by two HL ligands via the pyridyl N atom and the carbonyl O atom (Figure 1), and long axial interactions with perchlorate O atoms at a distance of 2.8098(15) Å. The protons on the amide N atoms, which do not coordinate to Cu in **1**, are hydrogen-bonded to the nearby perchlorate anions. The seven-membered rings formed by the chelating HL ligands are puckered slightly out of the N_2O_2 plane and serve to orient the amide NH groups away from the copper ion.

The bidentate N−O coordination mode is precluded when the ligand is deprotonated because the strongly coordinating amidate N ligand atom forms a chelate with the pyridyl group. When ligand L^- chelates to one metal through the pyridyl and amidate N atoms, it becomes impossible for the carbonyl O atom to form a bond to the same metal. The cluster complexes were synthesized from either cupric perchlorate hexahydrate or cupric triflate by combining the copper salt with HL and triethylamine in methanol. The complexes were formulated as $[Cu_8L_8(OH)_4]X_4$ (**2**X_4, X = ClO_4, OTf), on the basis of elemental analysis, mass spectroscopy, and X-ray crystallography. The hydroxide ions are incorporated into the structures presumably from water in the starting material and/or solvent in the case of cupric perchlorate hexahydrate, or from the solvent in the case of cupric triflate. X-ray crystal structures revealed that the cationic cluster portions of **2**$(ClO_4)_4$ and **2**$(OTf)_4$ are isostructural. A thermal ellipsoid representation of **2**$(ClO_4)_4$ is shown in Figure 2, and selected average bond lengths and angles for both **2**$(ClO_4)_4$ and **2**$(OTf)_4$ are listed in Table 2.

The highly symmetrical clusters are composed of four binuclear units of $[Cu_2L_2(OH)]^+$ (Figure 3a). Each binuclear unit contains two L^- ligands, one hydroxide ligand, and two copper(II) ions designated as CuA and CuB in Figure 3. The OH ligand bridges between CuA and CuB with Cu−O−Cu angles ranging from 119° to 130°. These relatively large angles contribute to CuA···CuB distances ranging from 3.33 to 3.46 Å. Many examples of hydroxide-bridged multinuclear copper complexes have been reported, particularly with respect to the relationship between the Cu−OH−Cu bond angle and the degree and type of magnetic exchange.[12,13] Hydrogen bonds (illustrated as dashed lines in Figures 2 and 3) between the hydroxide ligand and the carbonyl O atom further stabilize the binuclear pieces of the cluster.

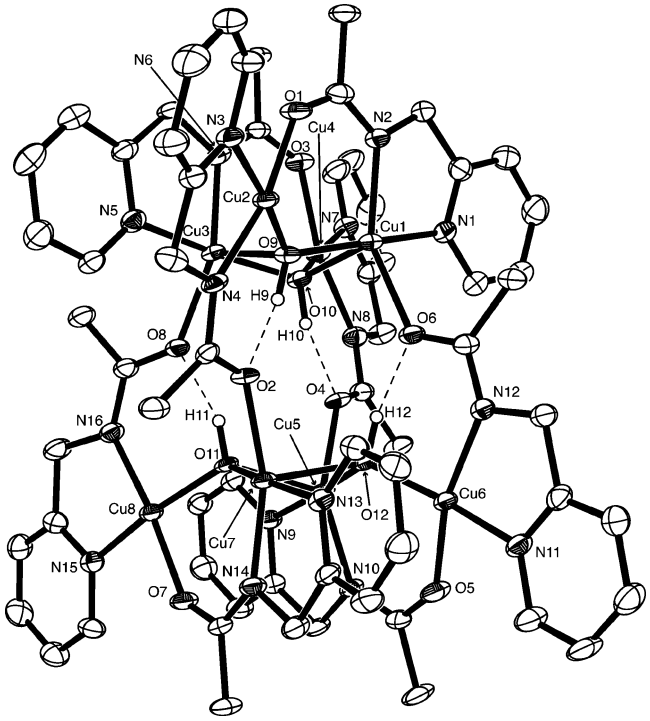

Figure 2. Representation of the X-ray crystal structure of $[Cu_8L_8(OH)_4](ClO_4)_4$, $\mathbf{2}(ClO_4)_4$; thermal ellipsoids are drawn at the 50% level. The perchlorate anions, solvent molecules, and all H atoms (except the hydroxide H atoms H9−H12) are omitted for clarity. Selected average bond distances and angles are summarized for $\mathbf{2}(ClO_4)_4$ and $\mathbf{2}(OTf)_4$ in Table 2.

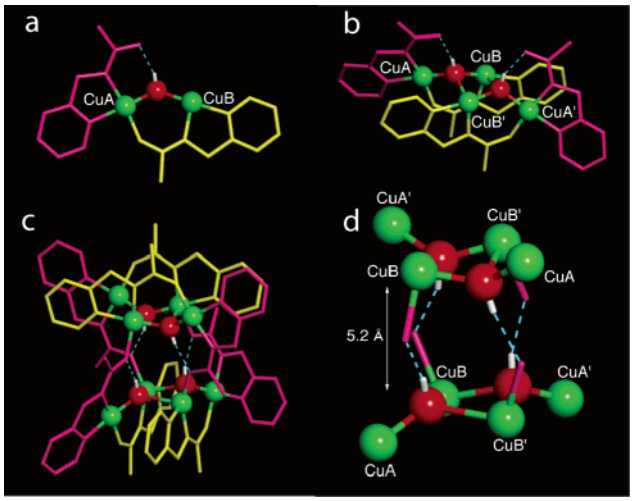

Figure 3. Ball and stick representations of $\mathbf{2}(ClO_4)_4$, with copper (green), hydroxide oxygen (red), syn-binding ligand (yellow), and anti-binding ligand (purple). (a) Binuclear $[Cu_2L_2(OH)]^+$ fragment, CuA−OH = 1.89−1.92 Å, CuB−OH = 1.91−1.94 Å, CuA−OH−CuB = 119−130°, CuA···CuB = 3.33−3.46 Å. (b) Tetranuclear $[Cu_4L_4(OH)_2]^{2+}$ fragment, CuB′−OH = 2.29−2.40 Å, CuB−OH−CuB′ = 95−98°, CuA−OH−CuB′ = 107−122°, CuB···CuB′ = 3.19−3.30 Å, CuA···CuB′ = 3.43−3.78 Å. (c) Full view and (d) the core of octanuclear $[Cu_8L_8(OH)_4]^{4+}$ cluster.

The L^- ligands coordinate to the copper ions via two slightly different modes. Half of the ligands (represented in yellow, Figure 3) coordinate to CuB via N atoms from the pyridyl ring and the amidate group, and via the carbonyl oxygen to CuA in a syn sense. The ligands binding in the syn sense, together with the bridging hydroxides, connect CuA and CuB to form the binuclear unit. The other half of the ligands (purple, Figure 3) coordinate to CuA via the N atoms, and to a symmetry-related CuB′ on the other side of the cluster via the carbonyl O atom in an anti sense. The two different bridging modes for ligand L^- allow for the self-assembly of the octanuclear clusters. Additional structural stability in the binuclear units is provided by hydrogen bonding between the hydroxide H atom and the carbonyl oxygen of the ligand binding in the anti conformation (see Figure 3a).

The rest of the cluster is related to the binuclear fragment through a noncrystallographic S_4 symmetry axis that runs through the center of the octanuclear cation. The C_2 symmetry axis relates the two binuclear fragments in the tetranuclear fragment shown in Figure 3b. The hydroxide ligands connect the binuclear pieces through the CuB atoms. The μ_3-OH groups thus bridge between CuA and CuB in the binuclear fragments, and between CuB and CuB′ in the tetranuclear fragments. The CuB···CuB′ distances are the closest copper−copper contacts in the structure, ranging between 3.19 and 3.30 Å. The average CuB−OH−CuB′ angles for $\mathbf{2}(ClO_4)_4$ and $\mathbf{2}(OTf)_4$ are 96(1)° and 97.9(3)°, respectively. These angles are very close to the singlet/triplet crossover angle for a θ value of 97.5° observed in oxo-bridged copper dimers.[11] However, the relationship between θ and J is more complex in hydroxo-bridged multinuclear copper complexes,[12,13] and our magnetic studies on $\mathbf{2}(ClO_4)_4$ revealed no correlation to the oxo-bridged examples (vide infra).

The coordination environments around CuA and CuB are square planar and square pyramidal, respectively. Both CuA and CuB are coordinated in their equatorial planes by the chelating pair of N atoms from the pyridyl and amidate groups on one ligand, a carbonyl O atom trans to the amidate N atom from a separate ligand, and a hydroxide ligand trans to the pyridyl N atom. In addition, CuB has an axial hydroxide ligand. The axial CuB−OH bond lengths are longer than the equatorial bond lengths for CuA−OH and CuB−OH (see Figure 3 caption) because of the expected Jahn−Teller distortions for d^9 copper(II).

The full octanuclear cluster is made up of two tetranuclear clusters related to each other via the pseudo-S_4 symmetry operation. The cluster shares the same symmetry that a tennis ball possesses, and the ligands on the top and bottom of the cluster can be viewed as the seams of the tennis ball. The two tetranuclear fragments are connected through the ligands binding in the anti conformation that bridges between the CuA and CuB atoms on either side of the cluster (Figure 3c). The distance between the copper ions in the top and bottom halves of the cluster is about 5.2 Å (Figure 3d).

Both $\mathbf{2}(ClO_4)_4$ and $\mathbf{2}(OTf)_4$ are soluble in acetonitrile, and although the predominant species in the electrospray mass spectra of acetonitrile solutions of $\mathbf{2}(X)_4$ is the binuclear fragment $[Cu_2(OH)L_2]^+$ with m/z = 441, both show the presence of the full cluster, $[\mathbf{2}(X)_3]^+$, at m/z = 2066.6 and m/z = 2214.9 for $[\mathbf{2}(ClO_4)_3]^+$ and $[\mathbf{2}(OTf)_3]^+$, respectively (Figure S1). The calculated isotope patterns for $[\mathbf{2}(ClO_4)_3]^+$ and $[\mathbf{2}(OTf)_3]^+$ match very closely the experimental isotope patterns observed (Figure S1 inset, Supporting Information). This clearly identifies the full eight-copper cluster as a

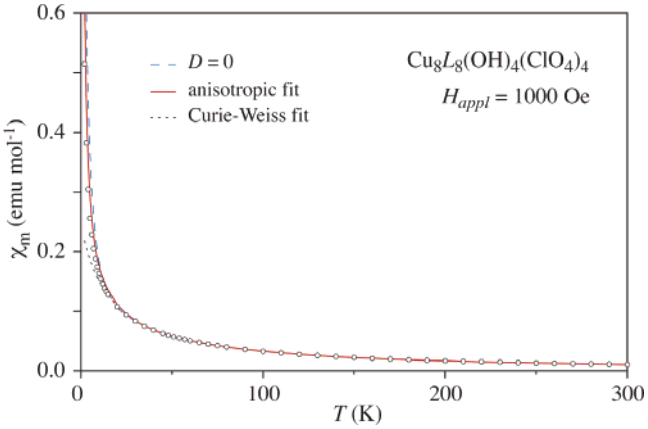

Figure 4. Magnetic susceptibility vs temperature for **2**$(ClO_4)_4$, measured in an applied field $H = 1000$ Oe. The fitting curves are described in the text.

component of the solution but does not directly show that the smaller fragments are present in solution. To address this question, we measured the conductances of solutions of **1** and **2**$(ClO_4)_4$. The slope of the Onsager plot for **1** is similar to other 1:2 electrolytes with pyridyl-containing ligands,[21] while the slope for **2**$(ClO_4)_4$ is greater, supporting the presence of a 1:3 or 1:4 electrolyte. A 1:3 electrolyte implies the 3+ cation $[Cu_6L_6(OH)_3]^{3+}$ and appears to be an unlikely explanation on the basis of the symmetrical structure of **2**$(ClO_4)_4$ and the absence of the $[Cu_6L_6(OH)_3]^{3+}$ species in the ESI-MS. A more reasonable explanation is that the full octanuclear cluster is present in solution and is in equilibrium with the tetracopper cluster, $[Cu_4L_4(OH)_2]^{2+}$. The presence of both the full octanuclear cluster and the tetranuclear cluster in solution would give rise to a conductance between a 1:2 electrolyte and a 1:4 electrolyte. Furthermore, the ^{1}H NMR spectra of **2**$(ClO_4)_4$ and **2**$(OTf)_4$ exhibit two methyl proton signals in an approximate ratio of 4:1. This result corroborates the notion that in solution the full octanuclear cluster is in equilibrium with the tetranuclear cluster and suggests an octanuclear-to-tetranuclear ratio of 2:1.

Frozen solutions of **2**$(ClO_4)_4$ and **2**$(OTf)_4$ are EPR-silent at 120 K, implying either diamagnetism or an integer spin system. Room temperature ^{1}H NMR spectra of **2**$(ClO_4)_4$ and **2**$(OTf)_4$ support the latter, having distinct paramagnetic shifts and broadening of the ligand proton signals. To further investigate the magnetic properties of **2**$(ClO_4)_4$, variable temperature magnetic susceptibility studies were conducted over the temperature range 2−300 K. The magnetization (M) was measured for a powder sample of **2**$(ClO_4)_4$ in an applied field of 1000 Oe (Figure 4). In these measurements, no difference was observed between field-cooled and zero-field-cooled measurements, indicating no magnetic ordering or single-molecule magnetic behavior in this temperature range. A fit above 30 K to a Curie−Weiss law, $\chi_m H = [C/(T - \theta) - \chi_D]$, with χ_D a T-independent diamagnetic term, is shown by the lower curve in Figure 4. This fit yields $\theta = -16$ K and $n_{eff} = 2.02$, using for C the Curie constant

$$C = 8\frac{N_A n_{eff}^2 \mu_B^2}{3k_B}, \qquad (1)$$

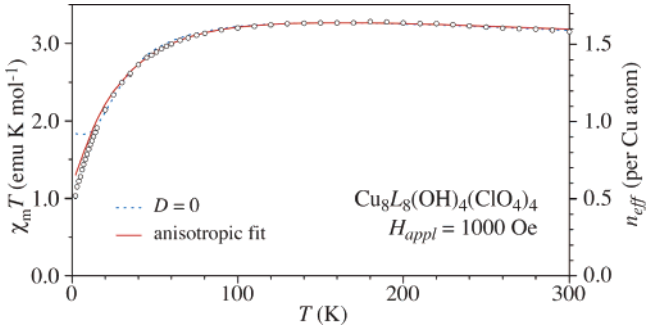

Figure 5. $\chi_m T$ product for **2**$(ClO_4)_4$, measured in an applied field of 1000 Oe. The theoretical curves are described in the text.

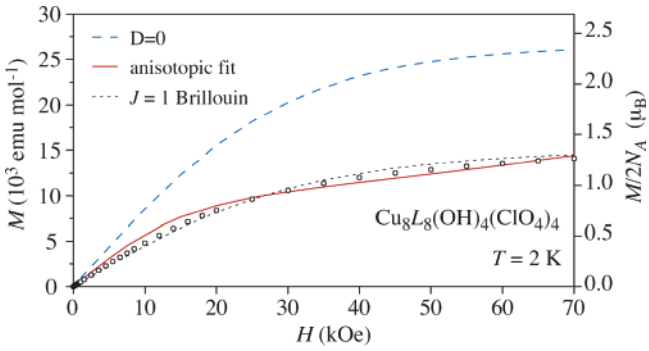

Figure 6. Magnetization measured vs applied field, at $T = 2$ K. At right is the moment calculated per four-Cu cluster (two clusters per molecule).

where the factor of 8 accounts for the number of Cu atoms per molecule. The effective Bohr magneton number $n_{eff} = 2.02$ exceeds the spin-only value 1.73 expected for Cu in the d^9 configuration; however, the excess (corresponding to $g = 2.34$) can be attributed to incomplete orbital quenching, and this falls at the upper end of range typically observed for Cu compounds.[24] The negative Weiss temperature indicates the Cu atoms to have magnetic interactions with a predominantly antiferromagnetic sign.

In Figure 5 is plotted the product $\chi_m T$ versus temperature, with an evaluation in terms of n_{eff} given for comparison on the right axis. It is clear that the effective moment is reduced at low temperatures, but not to zero as would be the case if the ground state were a nonmagnetic singlet. Rather, the reduction in n_{eff} is by a factor very close to 4, as can be seen from the low-temperature limit of Figure 5 (the diamagnetic term makes n_{eff} appear too small at high temperatures).

For further information about the magnetic interactions, the magnetization was measured in fields up to 70 kOe, at a fixed temperature of 2 K (Figure 6). Comparing these data to a Brillouin function showed that a curve corresponding to magnetic quantum number $J = 1$ appeared closest to the data, with a $J = 1$ fit (dotted curve in Figure 6) giving a saturation moment 2.72 per molecule, in units of μ_B. Since the susceptibility is proportional to $nn_{eff}^2 = ng^2J(J + 1)$, assuming n independent moments per molecule in the ground state (the factor 8 in eq 1), while the saturation moment per molecule is ngJ, n and g can be obtained independently from

(24) Orchard, A. F. *Magnetochemistry*; Oxford University Press: Oxford, 2003.

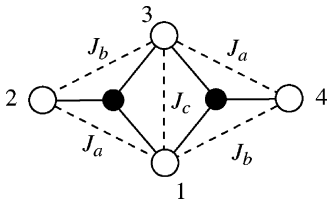

Figure 7. Model for the four-Cu cluster, with two bridging oxygen (●) joining four coppers (○). Three distinct exchange interactions are labeled.

the two measurements. From the 2 K value in Figure 5, we obtain $nn_{\text{eff}}^2 = 2.0$, which for $J = 1$ yields an unphysically small low-temperature value, $g = 0.37$. (With $J = {}^1/_2$, $g = 0.49$ is obtained this way.) Thus, although the Brillouin function agrees reasonably well in Figure 6, the data appear not to support a ground-state magnetic configuration consisting of isotropic multiplets.

The configuration of the $[Cu_8L_8(OH)_4](ClO_4)_4$ molecule is such that Cu atoms within the tetranuclear fragments are connected via the two bridging oxygens, with bond lengths (Table 2) indicating relatively strong connections between these atoms. Connections between the tetranuclear fragments are more indirect, with four bonds separating Cu atoms between subunits, and longer bond lengths along these pathways. Thus, we assume the tetranuclear fragment makes up the basic magnetic unit for this system. We have modeled this unit according to the scheme of Figure 7, where J_a, J_b, and J_c represent three distinct superexchange interactions, maintaining the 2-fold rotational symmetry of the molecule (see Figure 3b). Each of these interactions is mediated by a single oxygen bridge, while along the long axis of the cluster, we assume no coupling between Cu atoms labeled 2 and 4 (i.e., CuA and CuA′). This "butterfly" 4-spin configuration is similar to that of several Mn,[25−27] Fe,[28] V and Cr,[29] and Cu compounds.[30]

Assuming that the exchange interactions are isotropic, the Hamiltonian for this system can be written

$$\mathbf{H} = J_a(S_1 \cdot S_2 + S_3 \cdot S_4) + J_b(S_1 \cdot S_4 + S_2 \cdot S_3) + J_c(S_1 \cdot S_3) + DS_{\text{Tz}}^2 + g\mu_B H S_{\text{Tz}} \quad (2)$$

where the last term represents the Zeeman interaction, with S_{Tz} the operator corresponding to the z component of the total spin. (S_T is not a conserved quantity for the case where $J_a \neq J_b$.) The term containing D allows for an overall molecular anisotropy. For the case $J_a = J_b = J_{ab}$, the state energies can be solved directly, and these are shown in Table 3, where for $D \neq 0$ the energies are given in increasing order according to $S_{\text{Tz}} = 0$, $S_{\text{Tz}} = \pm 1$, and $S_{\text{Tz}} = \pm 2$ in the third column of the table. Examining the case $D = 0$, for $J_{ab} < 0$ and with $J_c < 0$ or with $J_{ab} \leftarrow |J_c|$, the "ferromagnetic" $S_T = 2$ state is the ground state. Alternatively, with J_c positive, the ground state consists of four degenerate states, an $S_T = 1$ triplet and an $S_T = 0$ singlet, for the following range of J_{ab}: $-J_c < J_{ab} < (J_c/2)$. In this situation, J_c dominates, forming a singlet between spins 1 and 3 (i.e., CuB and CuB′), while the remaining two spins are frustrated in the classic sense,[31] since despite the interaction J_{ab} these spins cannot find a preferred orientation, hence the degenerate ground state. For other combinations of J_{ab} and J_c, the ground state is a nonmagnetic singlet. The present case, having antiferromagnetic interactions and a reduced-moment magnetic ground state, matches most closely the frustrated degenerate configuration.

Table 3. Energies for the System of Equation 2 for the Case $J_a = J_b = J_{ab}$ and with $H = 0$

total spin	energy, $D = 0$	energies for $D \neq 0$
$S_T = 0$	$E = -({}^3/_4)J_c$	no D-dependence
$S_T = 0$	$E = ({}^1/_4)J_c - 2J_{ab}$	no D-dependence
$S_T = 1$	$E = -({}^3/_4)J_c$	$E = -({}^3/_4)J_c$, $-({}^3/_4)J_c + D$
$S_T = 1$	$E = ({}^1/_4)J_c - J_{ab}$	$E = ({}^1/_4)J_c - J_{ab}$, $({}^1/_4)J_c - J_{ab} + D$
$S_T = 1$	$E = ({}^1/_4)J_c$	$E = ({}^1/_4)J_c$, $({}^1/_4)J_c + D$
$S_T = 2$	$E = ({}^1/_4)J_c + J_{ab}$	$E = ({}^1/_4)J_c + J_{ab}$, $({}^1/_4)J_c + J_{ab} + D$, $({}^1/_4)J_c + J_{ab} + 4D$

For $D = 0$, the response of the system is isotropic, and in this case the magnetization can be solved analytically, using the van Vleck equation,[25] although we have solved the general case by direct numerical diagonalization of the Hamiltonian. The curves labeled "$D = 0$" in Figures 4−6 correspond to the isotropic situation with $J_c = 61$ K (42 cm^{-1}) and $J_{ab} = 0$. For this calculation, $g = 2.22$ provided good agreement at high temperatures; however, at low temperatures the effective moment, due to the degenerate triplet and singlet states, remains too large.

It is possible that magnetic interactions between four-Cu units may also be important, via the pathway Cu2−N4−C−O2−Cu7, and the three equivalent pathways corresponding to the pseudo-S_4 symmetry of the molecule. However, by the symmetry these interactions can be seen not to remove the frustration, and hence not to lift the degeneracy of the ground state. Alternatively, calculations for $D = 0$ but with $J_a \neq J_b$ showed that the ground-state singlet state becomes stabilized with respect to the triplet state, but with no change in the triplet-state g-factor. This yields an upward-curving M versus H graph, in disagreement with the data of Figure 6. Anisotropic exchange interactions can modify the g-factor for individual states by mixing states for different S_T,[32] and we made extensive trials for a model in which the exchange parameters J_a, J_b, and J_c were replaced by uniaxial tensors, all three having the same principal axes. Considerable reduction in ground-level g-factor could be obtained this way; however, the agreement for M versus H remained poor.

Much better agreement was obtained by the introduction of the molecular asymmetry parameter D of eq 2.[25] In this

(25) Vincent, J. B.; Christmas, C.; Chang, H.-R.; Li, Q.; Boyd, P. D. W.; Huffman, J. C.; Hendrickson, D. N.; Christou, G. *J. Am. Chem. Soc.* **1989**, *111*, 2086−2097.
(26) Libby, E.; McCusker, J. K.; Schmitt, E. A.; Folting, K.; Hendrickson, D. N.; Christou, G. *Inorg. Chem.* **1991**, *30*, 3486-3495.
(27) Basler, R.; Chaboussant, G.; Canada-Vilata, C.; Christou, G.; Mutka, H.; Janssen, S.; Altorfer, F.; Gudel, H.-U. *Polyhedron* **2003**, *22*, 2471−2479.
(28) McCusker, J. K.; Vincent, J. B.; Schmitt, E. A.; Mino, M. L.; Shin, K.; Coggin, D. K.; Hagen, P. M.; Huffman, J. C.; Christou, G.; Hendrickson, D. N. *J. Am. Chem. Soc.* **1991**, *113*, 3012−3021.
(29) Castro, S. L.; Sun, Z.; Grant, C. M.; Bollinger, J. C.; Hendrickson, D. N.; Christou, G. *J. Am. Chem. Soc.* **1998**, *120*, 2365−2375.
(30) Maspoch, D.; Ruiz-Molina, D.; Wurst, K.; Rovira, C.; Veciana, J. *Chem. Commun.* **2002**, 2958−2959.
(31) Toulouse, G. *Commun. Phys. (London)* **1977**, *2*, 115−119.
(32) Kahn, O. *Molecular Magnetism*; Wiley-VCH: New York, 1993.

case, with the field not aligned with the *z* direction, the Hamiltonian must be solved numerically. We found that, with $J_{ab} = 0$, good agreement was obtained using $J_c = 153$ K (106 cm^{-1}), $D = -39$ K (27 cm^{-1}), and $g = 2.17$, giving the red curves in Figures 4−6. In this calculation, we used the approximation that the magnetization powder average was given by the average of the values obtained with the field along the three principal axes, rather than a true powder integral. This will give some discrepancy at the highest fields; for example for a Mn 4-spin cluster, the true powder average was found to be about 10% lower than the principal-axis average in the high-field limit.[25] Investigation of situations with $J_a \neq J_b$ showed that good agreement with both the $M-T$ and $M-H$ data could be obtained over a range of J_a and $J_b < 30$ K (curves not shown).

For low fields in this model, the calculated effective moment remains somewhat higher than the observations as *T* goes to zero (Figure 5). The low-*T* magnetization is dominated by the $S_{Tz} = \pm 1$ doublet (or its equivalent for different sample orientations), split from the lowest triplet state due to the action of the *D* term. The *g*-factor of this doublet cannot be further lowered in this model, and so the small remaining discrepancy presumably indicates that a more complicated anisotropy should also be included, such as the tensor exchange interactions already described. However, we have not attempted to explore the entire phase space for this extended model. We believe that the isotropic model already described captures the most significant aspects of the magnetic behavior of this system, namely a frustrated magnetic system dominated by the antiferromagnetic interactions of spins 1 and 3 (CuB and CuB′), and a large molecular anisotropy. The anisotropy observed in the present case, $D = -39$ K, is large, for example 7−14 times larger than that observed in Mn clusters having the comparable butterfly geometry.[25,27] However, note that the relatively large *g*-factor identified here indicates a relatively large spin−orbit coupling in this case, which helps to explain the large observed anisotropy. For further comparison note that magnetic interactions of the Dzyalonshinskii−Moriya type[33] also rely upon spin−orbit coupling and have typical magnitude $J(g - 2)/g$, which is 26 K (18 cm^{-1}) in our case using the observed Curie−Weiss *g* value and $J = 106$ cm^{-1} already identified, while recent observations in copper benzoate[34] gave a magnitude of 20 K (14 cm^{-1}) for such interactions.

In summary, we have synthesized highly symmetrical copper hydroxide tennis ball clusters from simple polyfunctional ligands and copper salts. The coordination chemistry of the ligand is highly dependent on the amide proton, giving rise to monomeric **1** with the neutral HL, while producing the octanuclear clusters **2**$(ClO_4)_4$ and **2**$(OTf)_4$ when HL is deprotonated. The magnetic properties of the clusters are dominated by a frustrated magnetic system with antiferromagnetic interactions between the spins on CuB and CuB′ and a large molecular anisotropy. There is some structural similarity between the tetranuclear fragment illustrated in Figure 3b and the four-copper cluster in Cu_Z. The obvious potential of the clusters as preformed scaffolds for Cu_4S models of Cu_Z has focused our current efforts on **2**$(ClO_4)_4$ and **2**$(OTf)_4$ as starting materials toward this end.

Acknowledgment. We thank Ryan M. Sprouse (University of Oklahoma) and Lei Yang (University of Oklahoma) for preparing samples of **2**$(ClO_4)_4$, and Eric L. Klein (University of Oklahoma) for helpful discussions. We also thank Ewa Szajna (Utah State University) and Professor Lisa Berreau (Utah State University) for performing the conductance measurements on **1** and **2**$(ClO_4)_4$. This work was supported by the NSF (CHE-0094079 to R.P.H., DMR-0103455 to J.H.R.), the Herman Frasch Foundation (R.P.H.), the Welch Foundation (A-1526, J.H.R.), and Texas A&M University through the Telecommunications and Informatics Task Force (J.H.R.). Finally, we thank the NSF for the purchase of a CCD equipped X-ray diffractometer at the University of Oklahoma (CHE-0130835) and for the purchase of the SQUID magnetometer at Texas A&M University (NSF-9974899).

Supporting Information Available: X-ray data for **1**, **2**$(ClO_4)_4$, and **2**$(OTf)_4$ (CIF). Electrospray mass spectrum of **2**$(ClO)_4)_4$ (pdf). Additional figure. This material is available free of charge via the Internet at http://pubs.acs.org.

IC0493292

(33) Moriya, T. *Phys. Rev.* **1960**, *120*, 91−98.

(34) Zhao, J. Z.; Wang, X. Q.; Xiang, T.; Su, Z. B.; Yu, L. *Phys. Rev. Lett.* **2003**, *90*, 207204.